9th ANKARA INTERNATIONAL AEROSPACE CONFERENCE **AIAC-2017-103**
20-22 September 2017 - METU, Ankara TURKEY

INVESTIGATION OF THE EFFECT OF BOUNDARY CONDITIONS ON THE BUCKLING COEFFICIENTS OF STIFFENED FLAT PANELS

Enes Aydın[1]
Middle East Technical University
Ankara, Turkey

Altan Kayran[2]
Middle East Technical University
Ankara, Turkey

ABSTRACT

In this study, the effect of the boundary conditions on the buckling coefficients of stiffened flat panels is investigated utilizing finite element approach. In the first phase of the study, buckling coefficients of flat panels with classical boundary conditions are determined by finite element analysis and comparisons are made with the analytical solutions of the buckling coefficients provided in the literature. Very good agreement is obtained between the buckling coefficients determined by the finite element analysis and analytically determined buckling coefficients. In the second phase of the study, parametric finite element models are prepared via the script language for the selected skin-stringer combinations and linear buckling analyses are performed to determine the buckling coefficients of the selected skin-stringer combinations. The main objective of the study is to prepare a database for the buckling coefficients of the selected skin-stringer combinations and identify the differences between the buckling coefficients of the real skin-stringer geometries and the analytically determined buckling coefficients which rely on classical boundary conditions. Database prepared for skin-stringer assemblies with common J, Z and T type stiffeners are then processed to generate response surface (RS) and artificial neural network (ANN) which give the buckling coefficients as the output depending on the skin-stringer type. It is shown that ANN performs better than the RS for the 3 stringer types studied provided that overfitting is prevented via appropriate selection of the number of neurons which have to be decided iteratively case by case.

INTRODUCTION

Stiffened thin panels are very common and important structural elements in aerospace structures because of the weight and stiffness advantages they provide. Due to compressive stresses in the stiffened thin panel, thin panel may be buckled long before the limit load of the panel. Therefore, local panel buckling is usually allowed in the design of the aerospace structures. Once the critical buckling load is reached, the panel is incapable of supporting any further load [Mert, 2015]. Stiffeners carry the additional loads which come from the buckled panel. Hence, it is important to determine buckling load of the stiffened panels accurately.

[1] MSc Candidate in Aerospace Engineering Department, Email: e174677@metu.edu.tr
[2] Professor in Aerospace Engineering Department, Email: akayran@metu.edu.tr

In theory, buckling refers to the loss of stability of a component and it is commonly independent from the material strength. The theory of buckling is explained in-depth in the Theory of Elastic Stability [Timoshenko, 1936] which is considered as the classical book about buckling.

In the aerospace industry, stiffeners are designed to support panels when panel buckling is encountered. The stiffener section is important to determine the support condition that the stiffener provides on the unloaded edges of the panel. In the literature, analytical solutions obtained using classical boundary conditions allowed for the preparation of buckling coefficient charts with various loading conditions [Bruhn, 1973]. These charts also show the change in buckled shape as the boundary conditions are altered on the unloaded edges from free to fully restraint condition. Classical boundary conditions are commonly known as free, simply supported and clamped. In reality, neither simply supported nor clamped conditions are sufficient to describe the behavior of the true edge condition of stiffened panels, because the actual stiffener provides a condition which is in between these two. Therefore, buckling coefficient graphs provided in the literature are not sufficient to use effectively in aerospace structures which predominantly have stiffened thin walled panels. To have an optimum skin-stringer assembly design, the structure must be modelled with the correct boundary conditions. Moreover, finite element modelling and analysis of the actual skin-stringer assembly takes very long time in the design optimization process. In the literature, there have been several studies on the post-buckling behaviour of skin-stringer assemblies. In the study of Lync and Sterling [Lync and Sterling, 1998], a finite element methodology has been presented for the compressive post-buckling. In the study, test data are compared to results of four different finite element modelling approaches for the skin-stringer assembly. In the study of Weimin and his friends [Weimin, Mingbo, Liang and Dengke, 2008], experimental and analytical study results of post buckling simulation of an integral aluminum fuselage curved stiffened panel subjected to axial compression load has been presented. In the classical approach, in order to handle the non-uniform load over the skin panel after buckling, equivalent width concept has been used commonly [Bruhn, 1973]. Equivalent width pertains to the part of the skin that is assumed to carry uniform load. In the classical approach, effective width concept has been widely used in the post-buckling analysis of skin-stringer assemblies [Niu, 1999].

In this study, it is aimed to prepare a database for the buckling coefficients of selected skin-stringer combinations by means of parametric modeling via the script language followed by automated finite element analysis. With this approach, a database of buckling coefficients for skin-stringer assemblies can to be generated similar to the available buckling coefficient charts for the panels which have classical boundary conditions along the edges. In this study, skin-stringer assemblies are established for T, Z and J type stringers. In T and J type stringers, fasteners are used in double row arrangement. Using this database, the buckling load and the compression buckling coefficient of the skin-stringer assembly can be obtained much faster than modeling and analyzing the skin-stringer assembly by the finite element method. Thus, skin-stringer optimizations can be performed very quickly. In the present study, to construct the database, numerous skin-stringer assemblies are modeled with different sizes and types in Abaqus. Database is created by writing a script in Python which is then used in Abaqus to generate the parametric models of the skin-stringer assemblies followed by automated finite element analysis controlled by the Python script.

METHOD

Determination of buckling coefficients of panels with classical boundary conditions by finite element analysis

In the first phase of the study, buckling coefficients of flat panels with classical boundary conditions are determined by finite element analysis and comparisons are made with the analytical solutions of the buckling coefficients provided in the literature. This study is performed to gain confidence in the finite element analysis results. The geometry and the coordinate of the flat panel are presented in Figure 1. For a panel which is simply supported at 4 edges, boundary conditions at the edges are given in Table 1 [Muameleci, 2014].

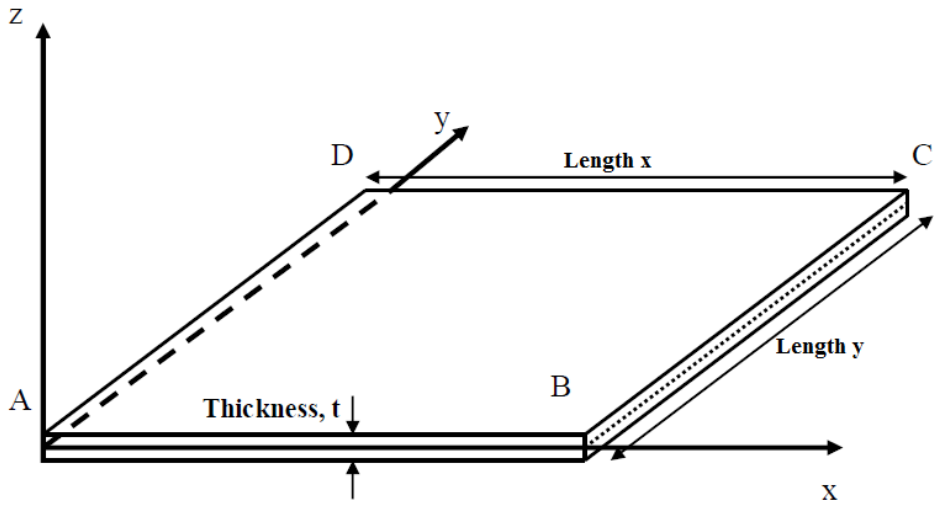

Figure 1: Definition of different geometrical parameters of the flat panels and the coordinate system

In Table 1, U1, U2 and U3 represent the translational degrees of freedom of the nodes in the x, y and z directions, respectively Similarly, R1, R2 and R3 represent the rotational degrees of freedom of nodes in the x, y and z directions, respectively.

Table 1: Definition of the constraints for the simply supported panel

Locations	U1	U2	U3	R1	R2	R3
Edge A to B			X			
Edge B to C			X			
Edge C to D			X			
Edge D to A			X			
Point A	X	X	X			
Point B						
Point C		X				
Point D						

Table 2 presents the boundary conditions for a panel which is clamped at four edges.

Table 2: Definition of the constraints for the clamped panel

Locations	U1	U2	U3	R1	R2	R3
Edge A to B			X	X		
Edge B to C			X		X	
Edge C to D			X	X		
Edge D to A			X		X	
Point A	X	X	X			
Point B						
Point C		X				
Point D						

For flat panels with different boundary conditions, a script is written in Python to model numerous panels with different sizes subject to different loading conditions such as compression or shear loading. Lowest eigenvalues obtained in the buckling analysis are used to calculate the buckling coefficients.

Critical buckling stress is calculated using Equation (1) [Bruhn, C5.2-C5.7, 1973],

$$\sigma_{cr} = \frac{\pi^2 * k * E_c}{12(1-v^2)}\left(\frac{t}{length\ y}\right)^2 \quad (1)$$

where t is the thickness of the panel, E_c is the compression elastic modulus of the panel material and factor k is the buckling coefficient which depends on the boundary conditions, geometric characteristic ($length\ x/\ length\ y$ ratio) and the loading condition (compression or shear). Compressive buckling coefficient curves are given in Fig. C5.2 [Bruhn, 1973] and shear buckling coefficient curves are given in Fig. C5.11 of the book by written by Bruhn [Bruhn, 1973].

In the finite element analyses, according to Figure 1, loading is applied in the x direction along edges AD and BC and the unloaded edges of the panel are AB and DC. The critical buckling stress is calculated using the lowest eigenvalue obtained in the buckling analysis performed in Abaqus as shown in Equation (2),

$$\sigma_{cr} = \frac{u_{FE}}{length\ x} * E_c * \lambda_1 \quad (2)$$

where u_{FE} is the applied displacement which is given as 1 mm in the x direction and λ_1 is the first eigenvalue obtained from finite element analysis.

By substituting Equation (1) into Equation (2), compression buckling coefficient is calculated as,

$$k = \frac{u_{FE}}{length\ x} * E_c * \lambda_1 * \frac{12(1-v^2)}{\pi^2 * E_c}\left(\frac{length\ y}{t}\right)^2 \quad (3)$$

To compare the finite element analysis results for the compression buckling coefficient with those provided by Bruhn [Bruhn, 1973], figures of buckling coefficients given by Bruhn are digitized to verify the FE results. Comparison of buckling coefficient versus plate aspect ratio curves are given in Figure 2-Figure 5, for different loading and boundary conditions.

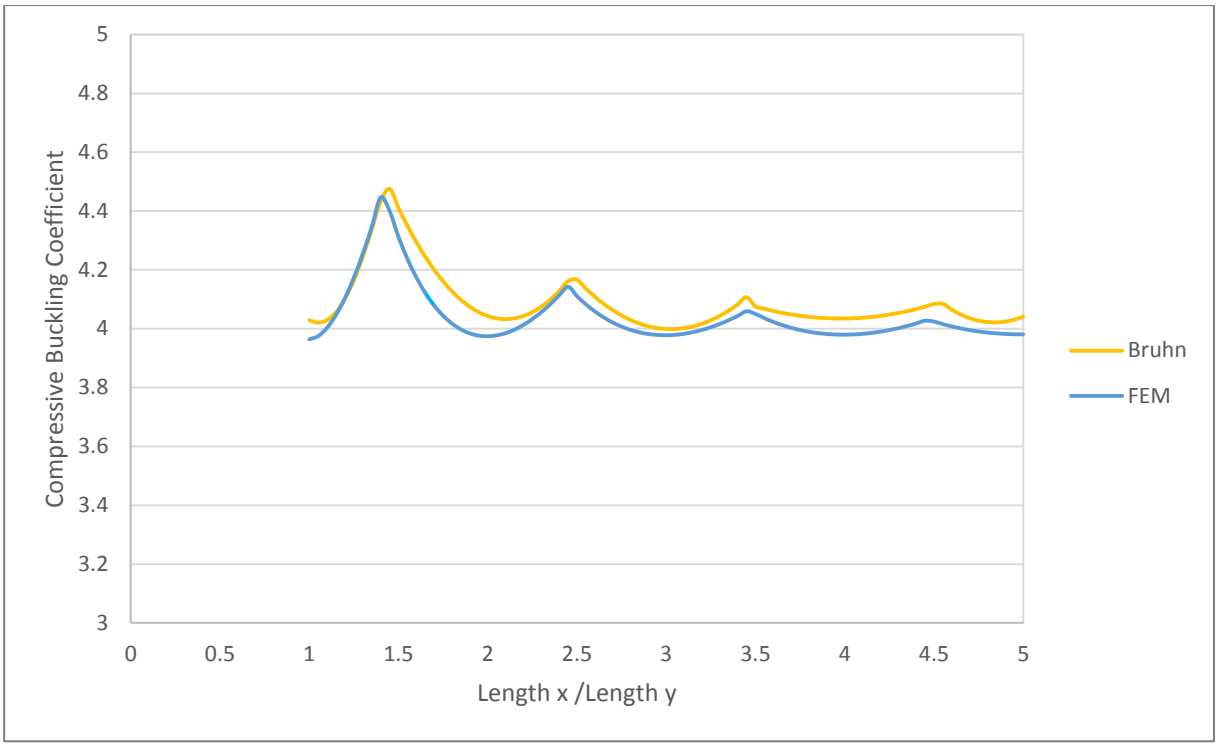

Figure 2 : Compressive buckling coefficients for flat rectangular panels with simply supported loaded and unloaded edges

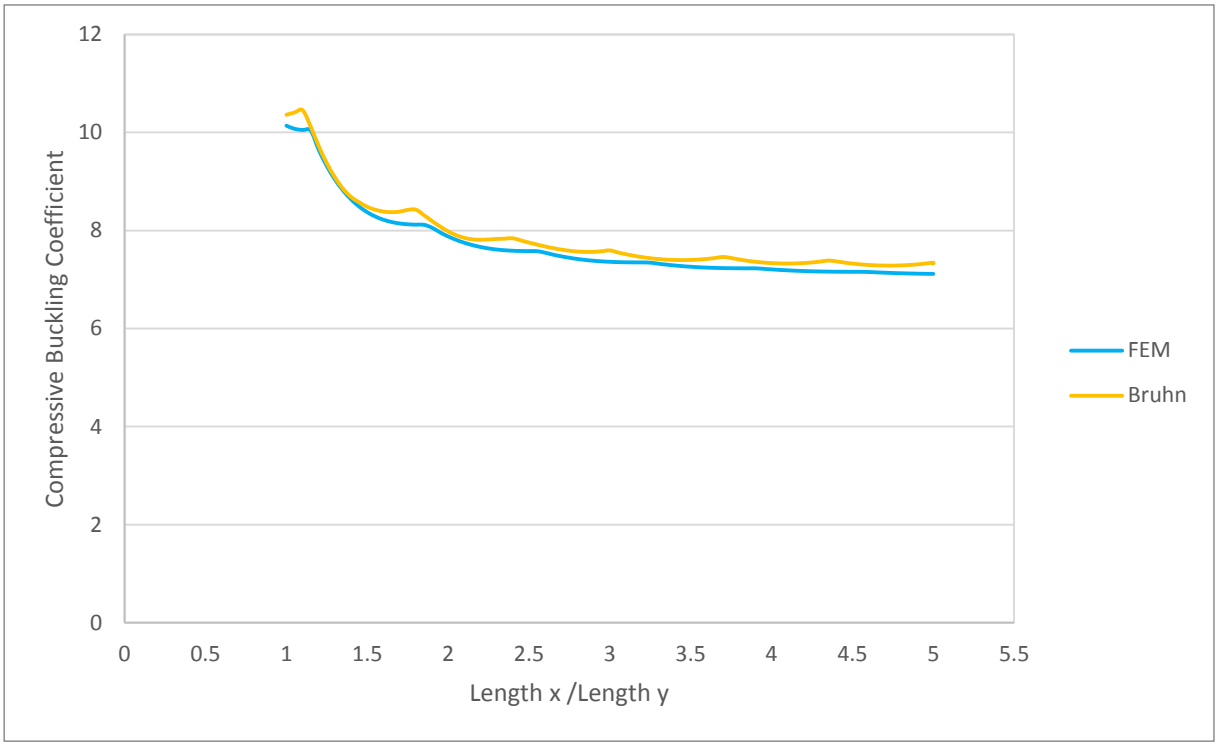

Figure 3 : Compressive buckling coefficients for flat rectangular panels with clamped loaded and unloaded edges

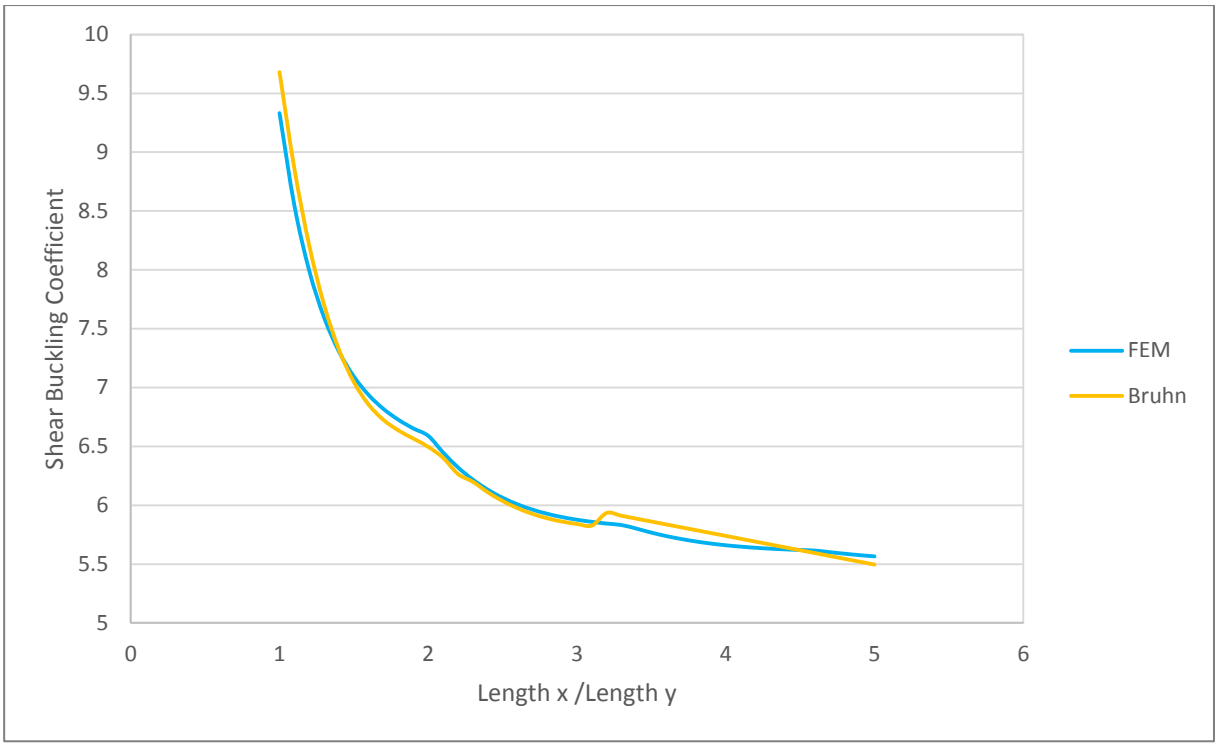

Figure 4 : Shear buckling coefficients for flat rectangular panels with simple supported loaded and unloaded edges

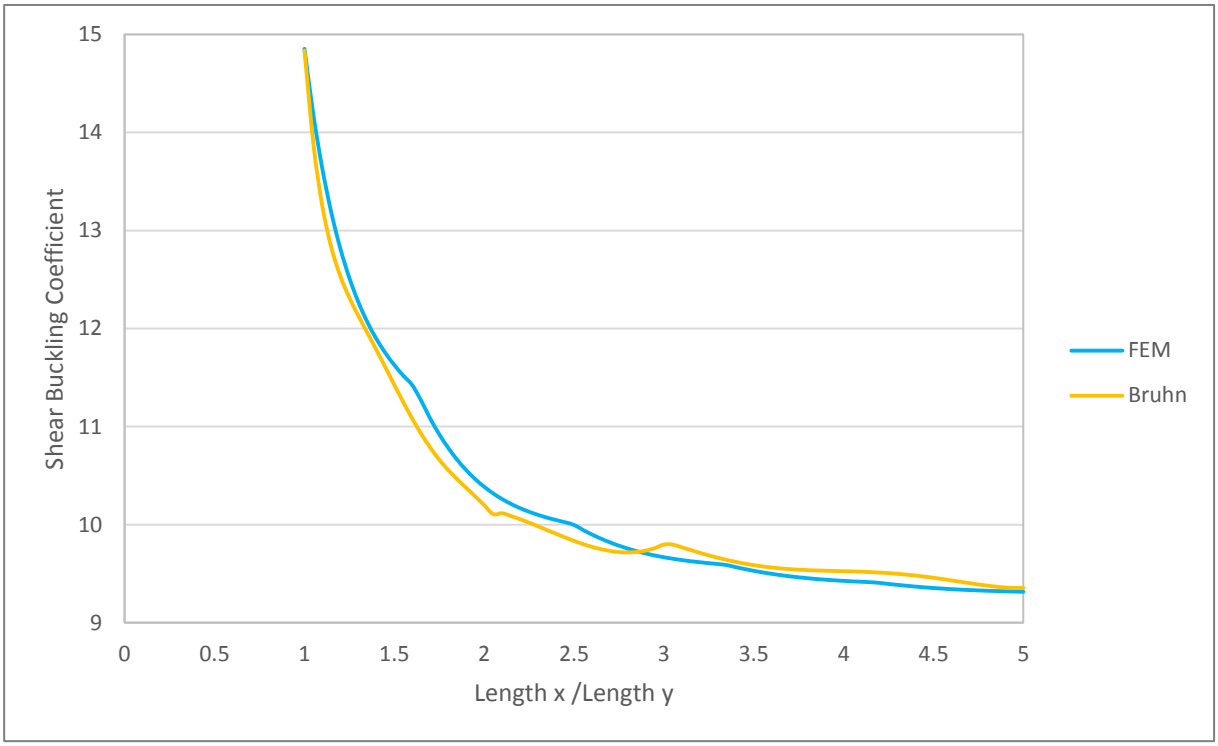

Figure 5 : Shear buckling coefficients for flat rectangular panels with clamped loaded and unloaded edges

It should be noted that the differences between the buckling coefficients obtained by the finite element analysis and analytically determined buckling coefficients provided by Bruhn are less than %1 in Figure 2-Figure 5. It is also noted that differences are mainly due to digitizing the plots given by Bruhn.

Determination of buckling coefficients of skin-stringer assemblies by finite element analysis

Following the verification of the boundary conditions of a single panel by the finite element analysis, stiffened panel modelling is performed using the verified boundary conditions along the loaded edges of the panel. However, for the stiffened panels, restraint along the unloaded edges is provided by the stiffeners on the panel. The boundary condition of loaded edges of skin-stringer assembly is considered as clamped edge condition.

The first skin-stringer assembly considered consists of three flat skin panels and two stringers with I cross section. Skin-stringer assembly and the skin panel numbering are demonstrated in Figure 6. Compression load is applied on the three skin panels from one of the edges along the y-axis as 1 mm displacement in the x direction. Figure 7 demonstrates the restraints applied to the loaded and the opposite edge of the panel. The degrees of freedom restrained along the loaded edge are U3 and R2. Along the other edge of the three skin panels, degrees of freedom U1, U3 and R2 are restrained. In addition, the middle edge of panel 2 is not allowed move in the y direction to avoid rigid body motion of the assembly, as shown in Figure 7. Moreover, unloaded side edges of the panels 1 and 3 are restrained in z-translation (U3 degree of freedom) and x-rotation (R1 degree of freedom).

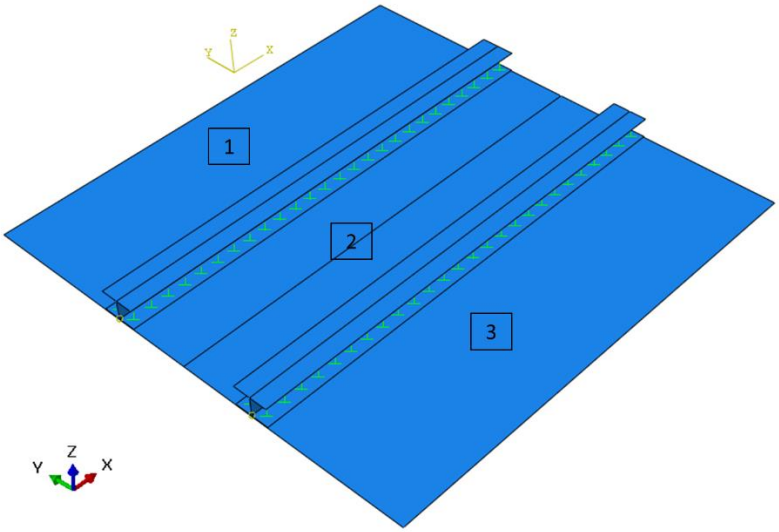

Figure 6 : Skin-stringer assembly analyzed

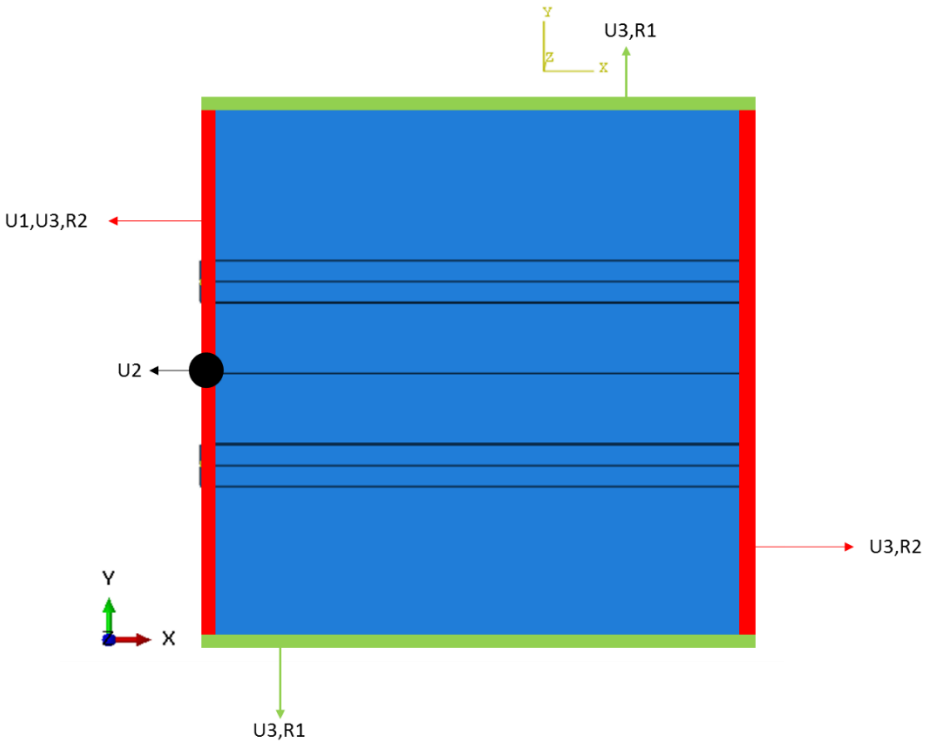

Figure 7 : Constraint configuration of skin-stringer assembly

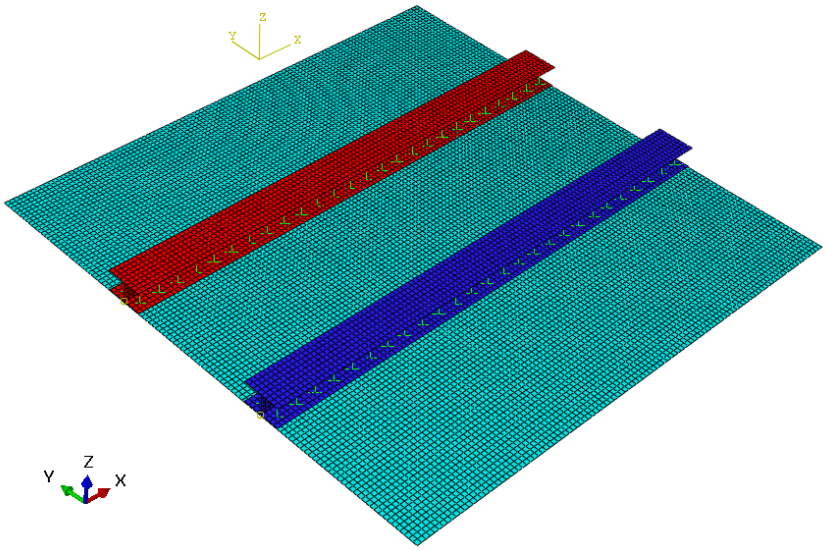

Figure 8 : Skin-stringer assembly with mesh

In the finite element model of the skin-stringer assembly, all stringers and skin panels are modelled as 2D shell elements with Aluminum 2024 T3 sheet material properties as shown in Figure 8. Stringers are connected to the skins by 3.2 mm diameter fasteners in double row arrangement. Fastener spacing is taken as 5 times the fastener diameter and fastener edge distance is the 2 times the fastener diameter plus 1mm as shown in Figure 9. These figures are commonly used in the aerospace industry.

Since it is too costly to model each fastener using its real geometry with a 3D model, fastener idealization is made. For this purpose, mesh-independent fastener is considered as a convenient method to define a point-to-point connection between two or more surfaces such as in a fastener connection. Thus, in the finite element model of the skin-stringer assembly, fasteners are modelled with the mesh-independent fastener module in ABAQUS.

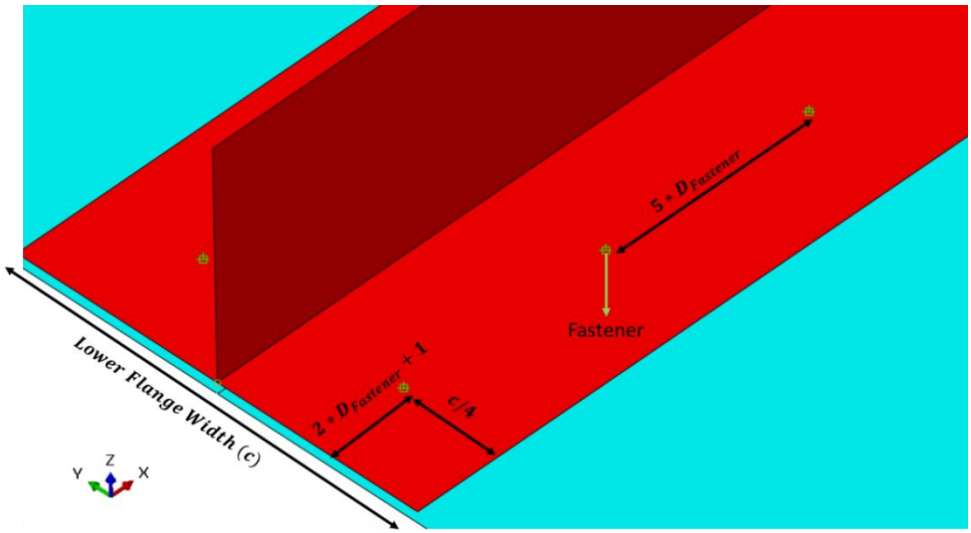

Figure 9 : Fastener pattern configuration

For the skin-stringer assembly, “Buckle” step of ABAQUS [Dassault Systèmes, 2010] is used to obtain the lowest buckling eigenvalue. Lowest eigenvalue is used in Equation (3) to calculate the compression buckling coefficient pertaining to the local buckling of the skin supported by the side stiffeners.

In the Result section, compression buckling coefficients calculated by the finite element solution are compared with the analytically determined compression buckling coefficient for the mid panel 2 in the skin-stringer assembly.

According to the model description made, a script is written Python 2.7 in order to create an ABAQUS finite element model, run the model and collect the lowest eigenvalue from the analysis results. In this study, most commonly used stringer sections Z, J and T are investigated as shown in Figure 10. The scripts are written for each skin-stringer assembly and the following parameters are specified by the user;

- Skin panel thickness
- Skin length y
- Stringer thickness
- Stinger height
- Stringer lower flange length
- Stringer upper flange length (In stringer section type T, there is no upper flange)

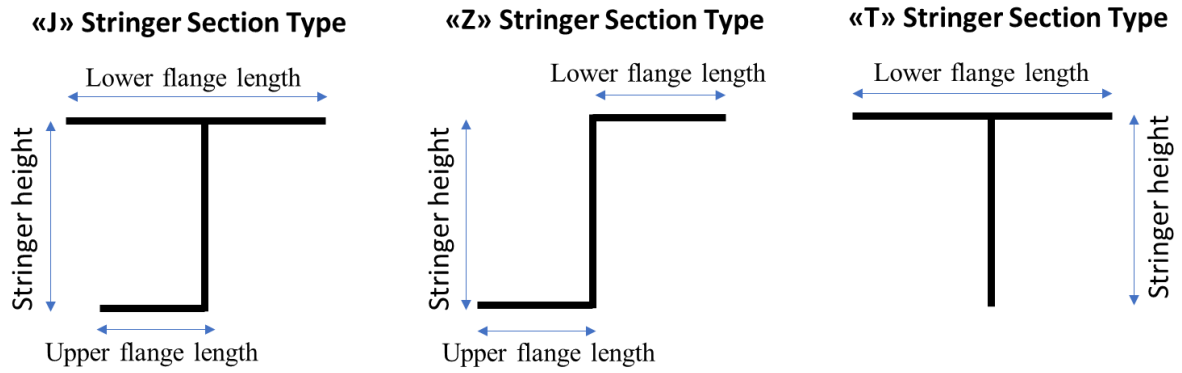

Figure 10: Stringer section types used in this study

To minimize the time and sources, some of the parameters of the skin-stringer assemblies are fixed to certain values as,

- Skin panel x = 450 mm
- Fastener diameter = 3.2 mm

- Material: Aluminum 2024 T3 Sheet

Discrete values of the design parameters of the skin-stringer assemblies are specified in a range. Upper and lower limits of the design parameters are decided based on the commonly used values in the industry.

For the skin-stringer assemblies with Z and J type stringers, the following parameters are specified between the upper and lower limits, and in total 2160 finite element analyses are performed to form a database for the buckling coefficients.

- Skin panel thickness = [0.813, 1.016, 1.27] mm
- Skin length y = [150.0, 225.0, 300.0, 375.0, 450.0] mm
- Stringer thickness = [0.813, 1.016, 1.27] mm
- Stinger height = [10.0, 17.0, 24.0 ,30.0] mm
- Stringer lower flange length = [10.0, 14.0, 18.0, 22.0] mm
- Stringer upper flange length = [10.0, 14.0, 18.0] mm

For the skin-stringer assembly with T section stringer, the following parameters are specified between the upper and lower limits, and in total 2100 finite element analyses are performed to form a database for the buckling coefficients.

- Skin panel thickness = [0.813, 1.016, 1.10, 1.27] mm
- Skin length y = [150.0, 225.0, 300.0, 375.0, 450.0] mm
- Stringer thickness = [0.813, 1.016, 1.10, 1.27] mm
- Stinger height = [10.0, 15.0, 20.0, 25.0 ,30.0] mm
- Stringer lower flange length = [10.0, 13.0, 16.0, 19.0 ,22.0] mm

To minimize the number of finite element analysis, for each parameter minimum number of discrete values are selected within the upper-lower limits of each parameter. Skin length y has a remarkable effect on the buckling phenomena. Hence, for the skin length y more number of discrete analysis points are used in the finite element analyses. However, for Z and J stringer section types, inner flange length is restricted to three values in order to minimize the number of analyses.

Setting up of artificial neural network (ANN) and response surface (RS) for fast determination of buckling coefficients

For fast determination of the buckling coefficients of skin-stringer assemblies with different stringer types, in this section artificial neural network and response surface are set up utilizing the finite element analysis results for the buckling coefficients. The output parameter, buckling coefficient, obtained from finite element analyses and input parameters of the skin-stringer assemblies are collected in an Excel file for the generation of the ANN and the RS for fast and accurate determination of buckling coefficients without resorting to finite element analysis. For the generation of the response surface, inputs and outputs are processed in MATLAB RSTOOL) [MATLAB Help, 2016]. Response surface model is chosen as “Full Quadratic”. In this study, full quadratic terms are used when the model of response surface is created. “Full Quadratic” terms consist of constant term, the linear terms, the interaction terms and the squared terms.

As the second fast and accurate analysis tool, an artificial neural network is established for each skin-stringer assembly by using the input parameters and the output parameter which is the buckling coefficient. Inputs and output of numerous analyses are processed in MATLAB NNTOOL to create an artificial neural network (ANN) [Yıldırım, 2015] [MATLAB Help, 2016]. For each type of stringer section, different ANN parameters are chosen to obtain accurate results. These parameters are neuron number, percentage of data sets used in the training set, percentage of data sets used in the validation set and percentage of data sets used in the test set. According to these parameters, performance of network is measured based on the mean squared error calculated using difference of ANN and FEM results.

The best network performance is obtained for J type stringer section for the following set of parameters:

- 8 Neuron number
- % 70 of the data set used in the training of the ANN
- % 15 of the data set used in the validation of the ANN
- % 15 of the data set used in the test of the ANN

Using these parameters in ANN, for the skin-stringer assemblies with J type stringer section, mean square error is calculated as 0.0238.

The best network performance is obtained for Z type stringer section for the following set of parameters:

- 6 Neuron number
- % 90 of the data set used in the training of the ANN
- % 5 of the data set used in the validation of the ANN
- % 5 of the data set used in the test of the ANN

Using these parameters in ANN, for the skin-stringer assemblies with Z type stringer section, mean square error is calculated as 0.0211.

The best network performance is obtained for T type stinger section for the following set of parameters:

- 6 Neuron number
- % 80 of data set used in the training of the ANN
- % 15 of data set used in the validation of the ANN
- % 5 of data set used in the test of the ANN

Using these parameters in ANN, for skin-stringer assemblies with T type stringer section, mean square error is calculated as 0.0307.

It should be noted that as presented in the Results section, buckling coefficients are in the range of 6-8 for the skin-stringer assemblies with J, Z and T type stringers. It is seen that for the 10 additional analyses for each stringer type, mean square errors are very small compared to the magnitude of the buckling coefficients. This shows that ANN approximation produces very accurate buckling coefficients which can be used reliably in the design process.

RESULTS

Calculation of buckling coefficients of skin-stringer assemblies

Preliminary study

Before presenting results obtained by the established artificial neural network and the response surface, a case study is performed for a panel with the loaded edges are considered as clamped as conditions and the unloaded edges closely simulating the clamped edge conditions with using stringer stiffness. Input parameters of this example assembly are shown in Table 3. The parameters given in Table 3 are decided iteratively such that with these parameters the unloaded edges simulate the clamped condition closely. The skin-stringer model is solved by using “Buckle” step of ABAQUS [Dassault Systèmes, 2010] for the lowest buckling eigenvalue as described in the Method section.

Table 3 : Input parameters of the skin-stringer assembly used in the finite element model

Skin panel material	Aluminum 2024 T3 Sheet
Skin panel thickness (mm)	0.91
Skin panel length x (mm)	450
Skin panel length y (mm)	150
Stringer material	Aluminum 2024 T3 Sheet
Stringer thickness (mm)	0.91
Stringer height (mm)	19
Stringer upper flange width (mm)	17
Stringer lower flange width (mm)	17

For the skin-stringer assembly specified in Table 3, the lowest eigenvalue is obtained as,

$$\lambda_1 = 0.1122 \tag{4}$$

Using this eigenvalue, the corresponding compressive stress and the compressive buckling coefficient are calculated as,

$$\sigma_{ccr} = \frac{u_{FE}}{length\ x} * E_c * \lambda_1 = 18.4517\ MPa \tag{5}$$

$$k_c = \sigma_{ccr} * \frac{12(1-v^2)}{\pi^2 * E_c}\left(\frac{length\ y}{t}\right)^2 = 7.3628 \tag{6}$$

If the skin panel 2 in Figure 2 is modeled with the same input parameters but classical clamped edge condition is assigned to the unloaded edges, for the panel aspect ratio of 3, compressive buckling coefficient is obtained from Figure 3 as 7.5941.

$$k_c = 7.5941 \tag{7}$$

In this example, it is seen that for the skin-stringer assembly defined in Table 3, the unloaded edge of panel 2 closely simulates the clamped edge condition. However, depending on the stringer type and how the stringer is connected to the skin, buckling coefficients obtained from the finite element analysis may or may not agree with the buckling coefficients obtained from pure analytical study utilizing the classical boundary conditions.

Comparison of buckling coefficients of skin-stringer assemblies determined by FEA, Response Surface and Artificial Network

Buckling coefficients of skin-stringer assemblies with J type stringers

Table 4 shows the input parameters of 10 additional analyses for the determination of buckling coefficients of skin-stringer assemblies. Parameters given in Table 4 are selected in between the parameters used in the finite element analyses specified in the Method section. Table 5 gives the finite element analysis (FEA), response surface (RS) and the artificial neural network (ANN) results.

Table 4: FEA input parameters for additional analyses for skin-stringer assemblies with 'J' type stringer

FEA	1	2	3	4	5	6	7	8	9	10
Skin panel thickness (mm)	1.05	0.85	1.2	1.2	1.15	1.05	1	0.9	1.1	1.15
Skin panel length x (mm)	450	450	450	450	450	450	450	450	450	450
Skin panel length y (mm)	350	200	325	320	400	275	200	175	235	325
Stringer thickness (mm)	1.1	1	1.2	1.25	1.2	1.07	1.03	1	1.15	1.2
Stringer height (mm)	18	13	28	25.5	17.5	16	19	18	22	23
Stringer upper flange width (mm)	15	12	17	16	15.5	11	13.5	10.5	15.5	16.5
Stringer lower flange width (mm)	16.5	15	17.5	17	15.5	12.5	14.75	11	15.75	17.75

Table 5: Buckling coefficients of skin-stringer assemblies with J type stringers / FEA results/ RS results / ANN results

#	FEA Results	RS Results	% Error (RS)	ANN Results	% Error (ANN)
1	7.57	7.684	1.51	7.561	0.12
2	7.14	7.162	0.31	7.091	0.68
3	7.74	7.627	1.46	7.734	0.07
4	7.72	7.623	1.26	7.739	0.25
5	7.66	7.871	2.75	7.612	0.63
6	7.00	7.054	0.77	7.091	1.30
7	7.05	7.042	0.11	6.989	0.86
8	6.85	6.887	0.54	6.881	0.46
9	7.12	7.250	1.83	7.107	0.18
10	7.57	7.662	1.22	7.648	1.03

For the skin-stringer assembly with J type stringer, Table 5 shows that the established ANN performs better than the RS. For the randomly selected 10 set of design parameters, root mean square (RMS) error with respect to the finite element results is 0.0494 for the ANN and 0.1048 for the RS.

Buckling coefficients of skin-stringer assemblies with Z type stringers

Table 6 shows the input parameters of 10 additional analyses for the determination of buckling coefficients of skin-stringer assemblies. Parameters given in Table 6 are selected in between the parameters used in the finite element analyses specified in the Method section. Table 7 gives the FEA, RS and the ANN results.

Table 6: FEA input parameters for additional analyses for stringer section type 'Z'

FEA	1	2	3	4	5	6	7	8	9	10
Skin panel thickness (mm)	1.05	0.85	1.2	1.2	1.15	1.05	1	0.9	1.1	1.15
Skin panel length x (mm)	450	450	450	450	450	450	450	450	450	450
Skin panel length y (mm)	350	200	325	320	400	275	200	175	235	325
Stringer thickness (mm)	1.1	1	1.2	1.25	1.2	1.07	1.03	1	1.15	1.2
Stringer height (mm)	18	13	28	25.5	17.5	16	19	18	22	23
Stringer upper flange width (mm)	15	12	17	16	15.5	11	13.5	10.5	15.5	16.5
Stringer lower flange width (mm)	16.5	15	17.5	17	15.5	12.5	14.75	11	15.75	17.75

Table 7: Buckling coefficients of skin-stringer assemblies with Z type stringers / FEA results/ RS results / ANN results

#	FEA Results	RS Results	% Error (RS)	ANN Results	% Error (ANN)
1	7.16	7.231	1.00	7.193	0.46
2	6.58	6.591	0.17	6.569	0.17
3	7.30	7.121	2.45	7.252	0.66
4	7.30	7.118	2.49	7.236	0.88
5	7.38	7.534	2.09	7.453	0.99
6	6.72	6.645	1.12	6.628	1.37
7	6.52	6.475	0.69	6.453	1.03
8	6.43	6.463	0.51	6.370	0.93
9	6.58	6.674	1.43	6.590	0.15
10	7.16	7.148	0.17	7.161	0.02

Buckling coefficient results obtained by the RS and the ANN for the additional 10 design sets again show that ANN performs better than the RS. For the randomly selected 10 set of design parameters, root mean square (RMS) error with respect to the finite element results is 0.0544 for the ANN and 0.1057 for the RS.

Buckling coefficients of skin-stringer assemblies with T type stringers

Table 8 shows the input parameters of 10 additional analyses for the determination of buckling coefficients of skin-stringer assemblies. Parameters given in Table 8 are selected in between the parameters used in the finite element analyses specified in the Method section. Table 9 gives the FEA, RS and the ANN results.

Table 8: FEA input parameters for additional analyses for stringer section type 'T'

FEA	1	2	3	4	5	6	7	8	9	10
Skin panel thickness (mm)	1.05	0.85	1.2	1.2	1.15	1.05	1	0.9	1.1	1.15
Skin panel length x (mm)	450	450	450	450	450	450	450	450	450	450
Skin panel length y (mm)	350	200	325	320	400	275	200	175	235	325
Stringer thickness (mm)	1.1	1	1.2	1.25	1.2	1.07	1.03	1	1.15	1.2
Stringer height (mm)	18	13	28	25.5	17.5	16	19	18	22	23
Stringer lower flange width (mm)	16.5	15	17.5	17	15.5	12.5	14.75	11	15.75	17.75

Table 9: Buckling coefficients of skin-stringer assemblies with T type stringers / FEA results/ RS results / ANN results

#	FEA Results	RS Results	% Error (RS)	ANN Results	% Error (ANN)
1	7.07	7.337	3.77	7.135	0.92
2	6.50	6.598	1.50	6.531	0.48
3	7.15	7.344	2.71	7.112	0.53
4	7.17	7.318	2.06	7.136	0.47
5	7.32	7.599	3.81	7.256	0.87
6	6.64	6.603	0.56	6.587	0.80
7	6.33	6.533	3.21	6.362	0.50
8	6.20	6.444	3.93	6.196	0.07
9	6.45	6.776	5.06	6.500	0.78
10	7.07	7.320	3.53	7.018	0.73

For the skin-stringer assembly with T type stringer, Table 9 shows that the established ANN performs better than the RS. For the randomly selected 10 set of design parameters, root mean square (RMS) error with respect to the finite element results is 0.0458 for the ANN and 0.2210 for the RS.

In these additional 10 analyses, it is seen that for the skin-stringer assemblies defined in Table 4, Table 6 and Table 8 for 'J', 'Z' and 'T' type of stringer sections difference between RS results and FEA results is not greater than 5%. RS gives fast convergence but this method does not give accurate results as the ANN. Difference between the ANN results and FEA results is not greater than 1.5%. However, ANN also has a problem with convergence. If the neuron number is increased too much, for instance over 10 for the buckling problem, overfitting occurs. It should be noted that when overfitting occurs, error on the training set is driven to a very small value, but when new data is presented to the network the error is large. Moreover, to get an accurate ANN many data sets are required. For the determination of the buckling coefficients, at least 2000 data sets are required to obtain reasonable results which are close to the finite element results with acceptable difference. Nevertheless, the established ANN can be used very effectively to determine the buckling coefficients of skin-

stringer assemblies with common J, Z and T type stiffeners. If desired ANN can be utilized to construct buckling coefficients charts similar to the buckling coefficient charts available for panel buckling with classical boundary conditions.

CONCLUSION

In this study, the effect of the boundary conditions on the buckling coefficients of stiffened flat panels is investigated by the finite element analysis. It is noted that depending on the restraint that the stringer along the unloaded edge of a skin-stringer panel provides, buckling coefficients obtained from finite element analysis may or may not agree with the buckling coefficients obtained by the analytical approach using the classical boundary conditions. For the skin-stringer assemblies with J, Z and T type stringers, buckling coefficients are determined by the finite element analyses for various combinations of the geometric properties of skin-stringer assemblies. Loaded edges of these assemblies are considered as clamped edge conditions. Finite element database for the buckling coefficients of skin-stringer assemblies for each stringer type is then processed to generate response surface and artificial neural network approximations. Response surface and neural network approximations allow very fast determination of the buckling coefficients of skin-stringer assemblies for the selected stringer types provided that the geometric properties of the skin-stringer assembly is are within the lower and upper limits of the geometric properties of the skin-stringer assemblies for which finite element analyses are conducted. To test the performance of the RS and the ANN generated, 10 additional random data sets are tested for each skin-stringer assembly with J, Z and T type stringer. It is seen that both the RS and the ANN methods give accurate buckling coefficient results compared to the FEA results. For the three stringer types, it is concluded that ANN gives more accurate results compared to the RS. However, it is noted that ANN also has accuracy problems if the parameters of the ANN are not selected appropriately. To select proper parameter set for the ANN, trial and error methodology is used. For instance, if the neuron number is lower than required neuron number, ANN gives inaccurate results. In addition, if the neuron number is higher than required neuron number, overfitting occurs in ANN. Therefore, required neuron number is decided with trial and error for each problem separately. Additionally, number of data sets is also very important in obtaining accurate ANN and RS. For the randomly selected 10 additional design sets, RMS values of the ANN 0.0494, 0.0544, 0.0458 for the skin-stringer assemblies with J, Z and T type stringers, respectively. It is to be noted that buckling coefficients are in the range of 6-8 for the skin-stringer assemblies with J, Z and T type stringers. For the 10 additional analyses for each stringer type, root mean square errors are very small compared to the magnitude of the buckling coefficients. This shows that ANN approximation produces very accurate buckling coefficients and it is deemed that such a fast and accurate approximate solver for the buckling coefficients based on ANN can be effectively used within the framework of optimization of skin-stringer assemblies.

References

Bruhn, E. (1973), *Analysis and Design of Flight Vehicle Structures*, 1973 Edition, Jacobs Publishing INC., p: C5-1 – C12-1, 1973.

Dassault Systèmes (2010), ABAQUS Analysis User's Manuel

Lynch, C. J., and Sterling, S. G., (1998), A Finite Element Study of the Postbuckling Behaviour of a Flat Stiffened Panel, International Council of the Aeronautical Sciences Congress, 1998.

MATLAB Help, 2016, "MATLAB 2016 Help", DC: Author. Retrieved from MATLAB 2016 Help Directory

Mert M. (2015), Post-Buckling Load Redistribution of Stiffened Panels in Aircraft Wingbox Structures, AIAC 2015, September 2015.

Muameleci, M. (2014), Linear and Nonlinear Buckling Analyses of Plates using the Finite Element Method, Linköping University, June 2014.

Niu, M.C.Y., (1999) Airframe Stress Analysis and Sizing, 2nd ed., Hong Kong CON., Indianapolis 1999, Chaps.11-14.

Timoshenko S.P. (1936), Theory of Elastic Stability, McGraw-Hill, Inc. New York 1936.

Weimin, S., Mingbo, T., Liang, G. and Dengke, D. (2008) Post-buckling Simulation of an Integral Aluminum Fuselage Panel Subjected to Axial Compression Load, Asia Simulation Conference-7th Intl. Conf. on Sys. Simulation and Scientific Computing, 2008.

Yıldırım A. (2015), Development of Bolted Flange Design Tool Based on Finite Element Analysis and Artificial Neural Network, Middle East Technical University, September 2015